NANO LETTERS

Letter

pubs.acs.org/NanoLett

Observation of Layer-Breathing Mode Vibrations in Few-Layer Graphene through Combination Raman Scattering

Chun Hung Lui,[†] Leandro M. Malard,[†] SukHyun Kim,[†] Gabriel Lantz,[†] François E. Laverge,[†] Riichiro Saito,[‡] and Tony F. Heinz*[,†]

[†]Departments of Physics and Electrical Engineering, Columbia University, 538 West 120th Street, New York, New York 10027, United States

[‡]Department of Physics, Tohoku University, Sendai 980-8578, Japan

Supporting Information

ABSTRACT: We report the observation of layer-breathing mode (LBM) vibrations in few-layer graphene (FLG) samples of thickness from two to six layers, exhibiting both Bernal (AB) and rhombohedral (ABC) stacking order. The LBM vibrations are identified using a Raman combination band lying around 1720 cm^{-1}. From double resonance theory, we assign the feature as the LO+ZO′ combination mode of the out-of-plane LBM (ZO′) and the in-plane longitudinal optical mode (LO). The LOZO′ Raman band is found to exhibit multiple peaks with a unique line shape for each layer thickness and stacking order. These complex line shapes of the LOZO′-mode arise both from the material-dependent selection of different phonons in the double-resonance Raman process and from the detailed structure of the different branches of LBM in FLG.

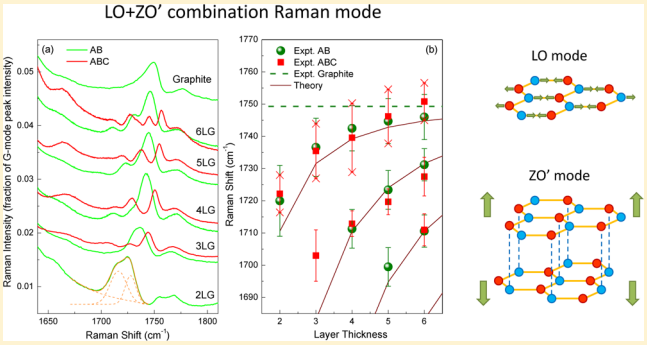

KEYWORDS: *Graphene, few layer, stacking order, layer-breathing mode, combination mode, Raman*

The low-energy electronic properties of few-layer graphene (FLG) and, correspondingly, the transport and infrared optical properties are largely defined by the interactions between the graphene layers. This topic has been the focus of much recent research. The influence of the interlayer interactions on the vibrational properties of FLG is also a subject of great interest. The different layer-breathing modes (LBMs), which involve out-of-plane relative displacement of individual graphene layers, are of particular importance because of their direct sensitivity to layer number and stacking order. Though LBMs have been characterized in bulk graphite[1,2] and multiwalled carbon nanotubes,[3,4] studied theoretically in FLG,[5−14] and reported in a recent experiment on trilayer graphene (3LG),[15] these modes have yet to be comprehensively investigated in FLG samples with different thickness and stacking sequences.

In this paper, we report the observation of LBMs in graphene samples with thickness from 2 to 6 layers with both Bernal (AB) and rhombohedral (ABC) stacking order. We observe this mode, which we designate as the ZO′ mode, through its signature in the LO+ZO′ combination Raman band formed with the in-plane longitudinal optical (LO) phonon. The measured LOZO′ frequency is found to shift with the photon energy (E_{exc}) of the excitation laser, a consequence of the selection of different phonon wave vectors in the electronically resonant two-phonon Raman process.[16−18] Comparison of the Raman dispersion with that of the two underlying phonons in the combination band provides a clear signature of the physical origin of the observed response. A striking feature of the LOZO′-mode is its marked sensitivity to both the layer thickness and stacking order of the FLG material. The LOZO′ Raman spectra for samples of each layer thickness and stacking order look qualitatively different from one another with multiple and distinct peaks over the range of thicknesses up to six layers examined this study.

We demonstrate that these spectroscopic features in the combination Raman mode reflect both the vibrational and electronic properties of FLG. For samples of thickness beyond bilayer, we observe multiple layer-breathing mode features with frequencies that depend both on the mode pattern (phonon branch) and sample thickness. These vibrations correspond to the different normal modes of a stack of graphene planes and can, as we show, be adequately described using nearest-neighbor harmonic couplings. In addition to these purely vibrational effects, the observed LOZO′ Raman spectra also reflect the electronic structure of the FLG samples. This dependence arises in a manner analogous to that of the 2D Raman mode in FLG.[15,17−19] Phonons of particular in-plane wave vectors are selected through the resonant Raman process

Received: July 2, 2012
Revised: September 5, 2012
Published: September 10, 2012

   dx.doi.org/10.1021/nl302450s | *Nano Lett.* 2012, 12, 5539−5544

in a way that depends on the electronic bands of the material. We identify this effect from measurements of the variation of the Raman spectra with the excitation photon energy (the Raman dispersion) and analyze it based on the electronic structure of the different samples. That the LOZO′ Raman spectra allow one to distinguish unambiguously the thickness and stacking order of FLG up to six layers is thus a reflection both of the inherently different character of the LBM vibrations and of sensitivity of the spectra to the electronic structure. As such, it extends and complements analysis using the 2D Raman response.[15,17−19] The approach also extends information available by measurement of the shearing mode phonons,[20] which has been observed through a single phonon process at very low Raman shifts. The shearing mode phonons also exhibit a strong dependence on layer thickness but are not expected to exhibit sensitivity to stacking, which arises for the two-phonon LOZO′ feature presented here by virtue of electronic resonance effects.

In our experiment, we investigated both pristine, mechanically exfoliated graphene layers that were freely suspended over trenches and samples deposited directly on fused quartz or SiO_2/Si substrates. We identified the layer thickness and stacking order by means of infrared spectroscopy[19,21−24] for graphene samples with layer number N = 1 to 6 exhibiting both AB and ABC stacking order. The Raman measurements were carried out under ambient conditions using a commercial (JY Horiba) confocal microRaman system over the spectral range of 1625 to 2100 cm^{-1}. We note that there were no systematic differences in the mode frequencies for the suspended and supported samples, although weak features were typically somewhat sharper and easier to identify for the suspended samples. (See Supporting Information for details of sample preparation, infrared and Raman measurement, and investigation of substrate effects.)

Figure 1 shows the Raman spectrum measured for free-standing graphene monolayers and bilayers (1LG, 2LG), as well as for bulk graphite.[15,25−27] The Raman intensity in this range is roughly 2 orders of magnitude smaller than that of the G mode.

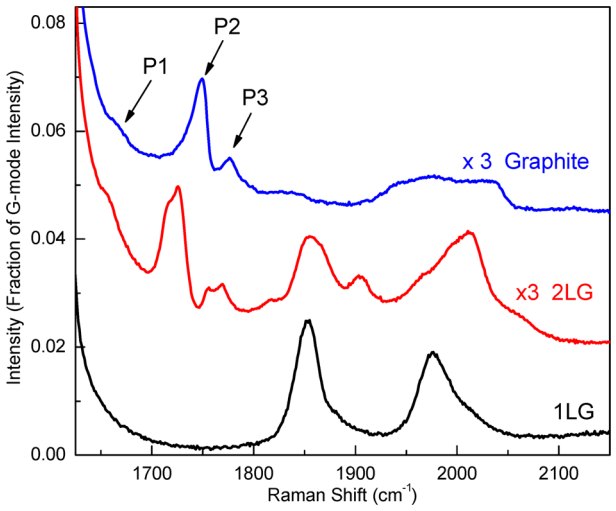

Figure 1. Raman modes in the range of 1625 to 2150 cm^{-1} for free-standing 1LG and 2LG, compared with bulk graphite for laser excitation energy E_{exc} = 2.33 eV. The spectra are normalized with respect to the G-mode peak intensity. The spectra of 2LG and graphite are increased by a factor of 3 in magnitude and displaced by 0.02 units for clarity.

We observe in graphite a weak (and as-yet unreported) Raman feature around 1655 cm^{-1} and two stronger peaks near 1730 and 1765 cm^{-1}.[25−27] We denote these peaks, respectively, as P1, P2 and P3. None of these three Raman peaks is observed from suspended 1LG or from 1LG supported on a quartz substrate[26,27] for different E_{exc}. As shown in Figure 2 for 2LG, the peaks exhibit Raman dispersion. While the frequency of P3 changes only slightly with the photon excitation energy E_{exc}, both P1 and P2 significantly blue shift with E_{exc} with average dispersions of 38 and 29 cm^{-1}/eV, respectively. As we describe below, we have applied double-resonance Raman theory[16−18,28] to analyze the dispersion behavior and to assign P1, P2, and P3, respectively, to the LO+ZA, LO+ZO′ combination modes, and to the 2ZO overtone mode by an intravalley resonant scattering process. Here LO and ZO′ denotes, respectively, the in-plane optical phonon modes and the out-of-plane interlayer breathing modes (see Figure 2c for their atomic displacements), and ZA and ZO denote, respectively, the out-of-plane acoustic and optical modes of a graphene layer, near the Γ point in the Brillouin zone. We note that in the double-resonant overtone and combination Raman modes, the Raman shift corresponds to the sum of the frequencies of the two underlying phonons, which carry equal (but opposite) in-plane momentum. The interlayer optical modes measured here are therefore not strictly rigid-plane modes, but modes with undulation in the graphene plane from the finite in-plane wave vector. With the above assignments, the absence of features P1, P2, and P3 in 1LG can be readily understood: the ZA and ZO mode are not Raman active in 1LG,[8] while the LBM (ZO′) obviously requires more than one graphene layer. We focus on the LOZO′ feature and ZO′ mode in this paper; the newly identified LOZA and 2ZO modes are discussed in the Supporting Information.

To analyze the LOZO′ response (feature P2) in 2LG, we investigated the phonon dispersion of the LO and ZO′ branch experimentally by directly measuring their overtone modes (2LO and 2ZO′) (see Supporting Information). Both overtone modes exhibit dependence on E_{exc} arising from the double-resonance Raman scattering mechanism. In particular, we observed two components ($2ZO'^{+}$ and $2ZO'^{-}$) in the 2ZO′ line, which we attribute to resonances between different electronic bands in 2LG. Figure 2b shows the LO and ZO′ phonon energies, obtained as half of their overtone values. We found that the combination of a LO phonon and a ZO′ phonon matches well with the frequency and dispersion of feature P2. Figure 3a displays the ZO′ phonon energies obtained by subtracting the LO phonon energies from the LOZO′-mode energies as a function of phonon momentum. The results are compared with published theoretical predictions[12] and with the ZO′ phonon energies obtained from the 2ZO′ overtone mode. The good agreement with both the experimentally and theoretically derived values confirms our assignment of P2 as the LOZO′ combination mode. (Figures 2 and 3a also display the results of similar analyses of LOZA and 2ZO modes with detailed discussion provided in the Supporting Information.) Our assignment is also consistent, both in terms of the Raman shift and dispersion characteristics, with a recent theoretical calculation of the LOZO′ spectra using the double-resonance Raman theory.[13]

Since the LOZO′ mode involves the layer-breathing vibrations, its behavior should, of course, be sensitive to interlayer interactions. To explore this issue, we measured the LOZO′ line for graphene samples of layer thickness N = 2 to 6

dx.doi.org/10.1021/nl302450s | Nano Lett. 2012, 12, 5539−5544

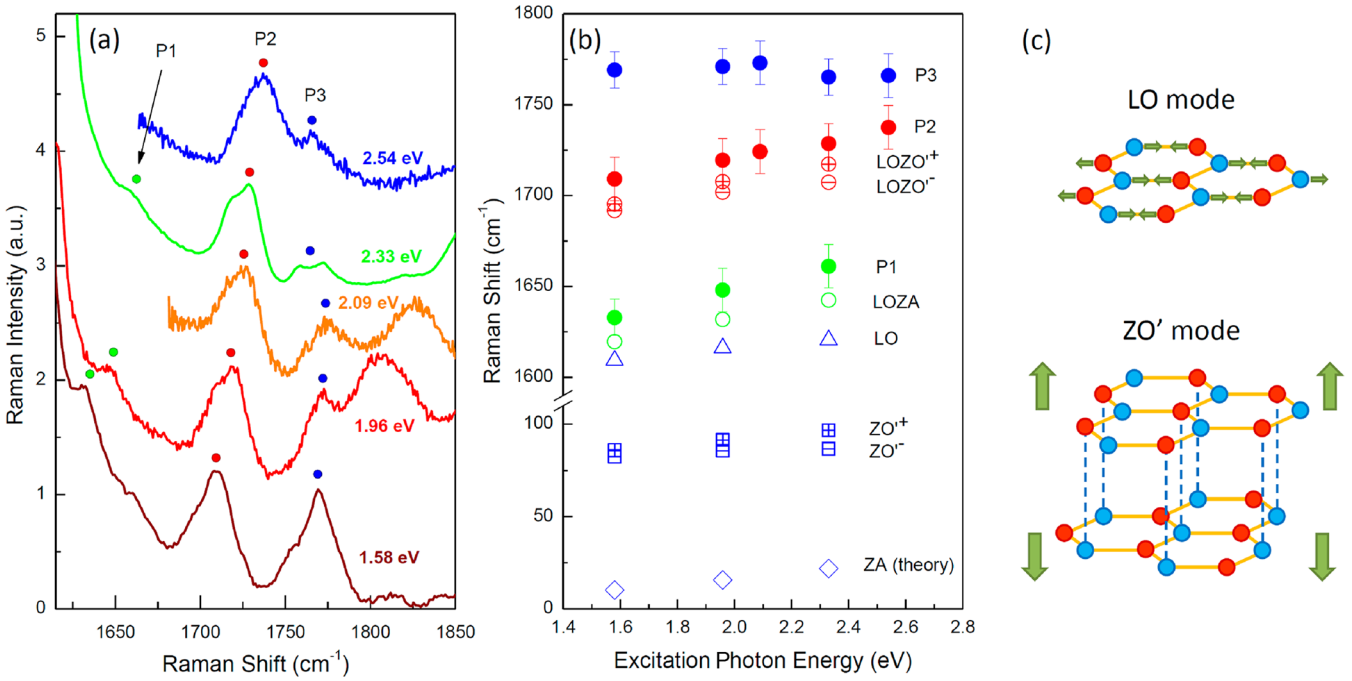

Figure 2. (a) Raman spectra of 2LG (displaced for clarity) in the range of 1615 to 1850 cm^{-1} for different laser excitation energies E_{exc}. For E_{exc} = 1.96 and 2.33 eV, the measurements were performed on free-standing 2LG; for the other cases, the other samples were supported on fused quartz substrates. Note that the strongly dispersing LO+TA band[26,27] (at 1810 cm^{-1} for E_{exc} = 1.96 eV) overlaps with P3 for E_{exc} =1.58 eV. (b) The frequency (solid dots) of different Raman peaks as designated in (a) as a function of E_{exc}. The circles are comparisons based on the appropriate combination of the different component phonon modes in the LOZO′ mode. The LO and ZO′ phonon frequencies were determined experimentally from their overtone modes. The diamonds are theoretical values of ZA phonon frequency from Figure 3a. (c) Schematic diagrams of the atomic displacement of the LO and ZO′ phonon modes of 2LG at the Γ point of the Brillouin zone. The red and blue dots represent the A and B sublattices in the graphene honeycomb structure.

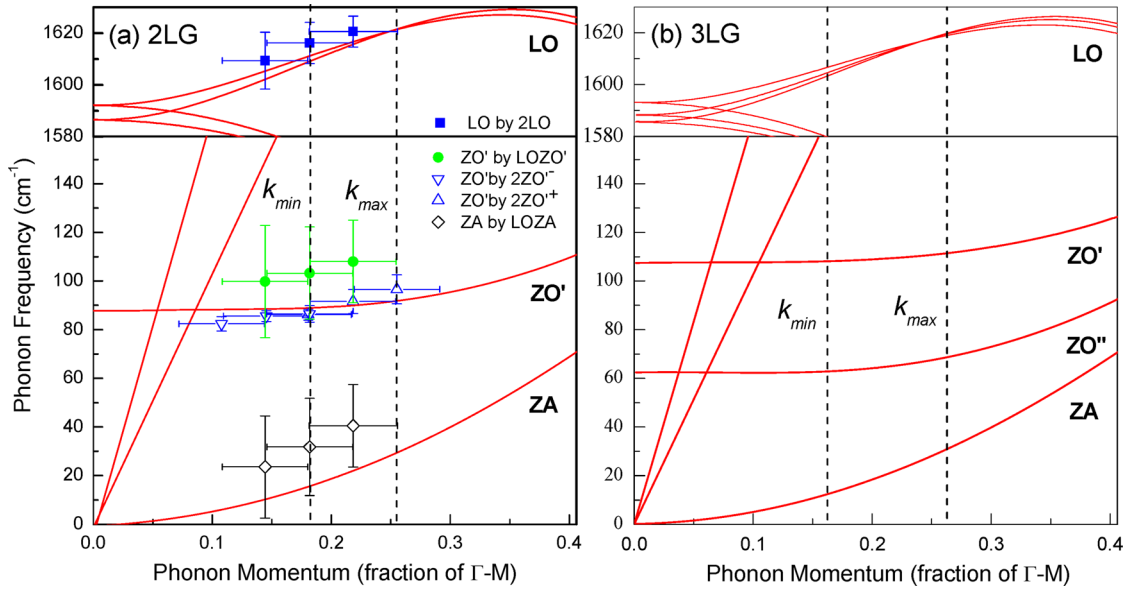

Figure 3. (a) Comparison of experimental (symbols) and theoretical (lines) frequencies for the LO, ZO′, and ZA modes in 2LG. The LO (squares) and ZO′ (triangles) phonon frequencies were determined experimentally from their overtone modes. The ZO′ (dots) and ZA (diamonds) phonon frequencies were obtained by subtracting the LO phonon frequencies (squares) from the measured LOZO′- and LOZA-mode frequencies, respectively. The errors bars represent uncertainties defined by the width of the Raman lines. The phonon momenta for the experimental points are taken as the average transition momenta in 2LG with the error bars representing the uncertainties arising from various resonant Raman scattering processes (see Supporting Information). (b) Same as (a) for 3LG. We here neglect the next-nearest-layer interaction and assume the phonon band structure to be the same for ABA and ABC trilayers. In both (a) and (b), the theoretical curves for LO modes are from ref 6, while those for low-energy modes are from ref 12. The dashed lines are representative phonon momenta in the double-resonance processes for 2LG and 3LG at E_{exc} = 2.33 eV, as described in the text.

dx.doi.org/10.1021/nl302450s | Nano Lett. 2012, 12, 5539−5544

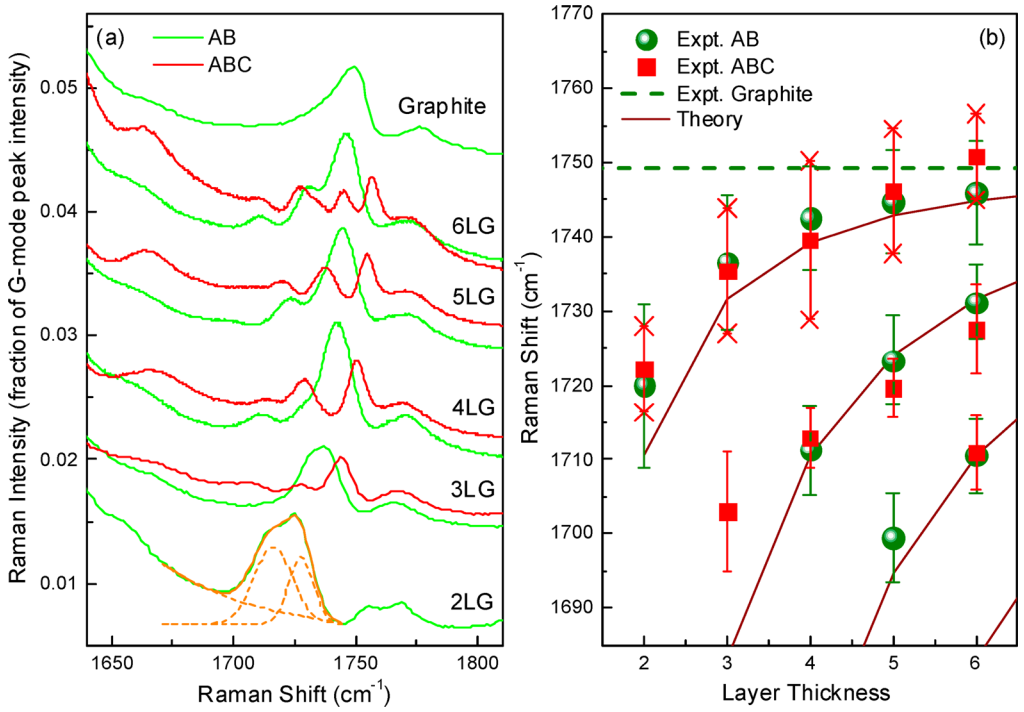

Figure 4. (a) Raman spectra in the range of 1640 to 1810 cm^{-1} for FLG of different thickness and stacking order with E_{exc} = 2.33 eV. We used free-standing 2LG, when available. For thicker FLG, the samples were supported on SiO_2/Si substrates. The spectra are normalized with respect to the G-mode peak intensity. The orange lines represent a double-Gaussian fit for the 2LG LOZO′ peak. (b) The energy of the subpeaks in the LOZO′ band for FLG with two stacking orders as a function of layer thickness. The error bars correspond to the width of the Raman features. For the high-energy peaks of the ABC spectra, we present the average values of the two highest energy peaks. The positions of the original peaks lie at the ends of the corresponding error bars. For 2LG, the green dot is the average energy, and the red crosses and squares are, respectively, the peak positions of the two Gaussian components and their average value. The lines are the calculated frequencies $\omega_n(N)$ of the LBM phonons based on the nearest-neighbor coupling model as described in the text and upshifted to match the experimental value for bulk graphite (dashed line).

(2LG to 6LG) with both AB and ABC stacking sequence (Figure 4a). The LOZO′ band exhibits multiple peaks for all samples. The positions of the subpeaks of the LOZO′ band evolve systematically, increasing from 2LG to 6LG. Representing the frequency by the centroid of the LOZO′ band, we find that the average frequency for FLG with AB (ABC) stacking increases by 18 cm^{-1} (22 cm^{-1}) from 2LG to 6LG and approaches (slightly exceeds) the value of the bulk Bernal graphite. The in-plane LO mode is essentially unchanged by interlayer coupling.[6] Consequently, the observed layer-dependent behavior of the LOZO′ mode is expected to reflect the behavior of the LBM (ZO′), which is clearly sensitive to the layer thickness, as well as the influence of the electronic resonance condition, as discussed below.

In addition to the layer-dependent behavior, the LOZO′ mode also exhibits strong sensitivity to the stacking sequence (relevant for N = 3 to 6). For AB-stacked samples (Figure 4a), the peak at the highest frequency is significantly stronger than the other subpeaks. As N increases, the number of subpeaks increases and their positions shift toward the main peak. In contrast, the spectra for ABC-stacked graphene (Figure 4a) generally exhibit a greater number of peaks with narrower line widths and more evenly distributed spectral weight than the AB spectra. The energies of peaks in the ABC spectra also differ somewhat from those in the AB spectra. Such distinctions between the AB and ABC spectra are found to persist for all photon excitation energies E_{exc}. (See, for example, the case of 3LG in the Supporting Information.)

The sensitivity of the Raman LOZO′ spectrum to layer number and stacking order arises from two factors. First, the distinct electronic structure of different FLG samples influences the Raman response through the selection of different phonon wave vectors by the double resonance process. This mechanism is responsible for the layer and stacking-order dependence of the line shape of the 2D Raman mode.[15,17−19] Second, the layer thickness and stacking order of the FLG directly affect the ZO′ modes in the material and, hence, alter the characteristics of the LOZO′ band. In particular, for N-layer graphene, there are $N-1$ distinct ZO′ modes (which we label as $ZO'^{(1)}$, $ZO'^{(2)}$ ... $ZO'^{(N-1)}$), each with a different frequency. These branches can be considered to correspond (in the absence of in-plane momentum) simply to the normal modes of N sheets of graphene, each free to oscillate rigidly in the perpendicular direction. As is intuitively clear and discussed below in further detail, the frequencies of the set of different modes depend strongly on the layer thickness. Thus, in contrast to the case of the 2D mode,[15,17−19] where the underlying in-plane phonons are essentially identical for different layer thicknesses and the sensitivity of the Raman response arises from the variation of the electronic structure, the strong dependence of the LOZO′ Raman response to the thickness of FLG also reflects the inherent differences of the LBM phonons being probed. This behavior is analogous to that of the other interlayer vibration, that associated with the shearing mode.[20]

To clarify the roles of electronic and direct vibrational effects in defining the LOZO′ Raman spectra, let us first analyze the behavior of 2LG in detail. We see that the LOZO′ spectrum exhibits a somewhat complex line shape with a pair of peaks at 1716 and 1727 cm^{-1} (Figure 4a). These two peaks do not arise from the phonon band structure: 2LG has only one LBM and

dx.doi.org/10.1021/nl302450s | Nano Lett. 2012, 12, 5539−5544

the splitting of the two branches of the LO mode induced by interlayer interactions is very slight (~2 cm^{-1}).[6] We therefore examine the different possible electronic processes for resonant Raman scattering to explain the observed LOZO′ spectrum. For this purpose, we treat the 2LG electronic structure within a simple tight-binding model, including only the dominant intralayer (γ_0) and interlayer (γ_1) couplings. We can then determine the minimum (k_{min}) and maximum (k_{max}) phonon momenta (Figure 3a) for resonant processes at E_{exc} = 2.33 eV through intraband scattering within the low- and high-lying conduction (valence) bands. (See Supporting Information for details.) Using these two momenta and the theoretical phonon dispersion relations in Figure 3a, we find the energies for the corresponding LO+ZO′ phonons differ from one another by ~15 cm^{-1}. This figure is comparable to our experimentally observed separation of 11 cm^{-1} between the two LOZO′ components. We therefore ascribe the two peaks in the LOZO′ mode of 2LG to different electronic resonances in the two-phonon Raman scattering processes.

The same mechanism appears to be responsible for some of the structure in the LOZO′ band in ABC stacked 3LG (Figure 4a). In this case, the spectrum exhibits three peaks, separated from one another by ~20 cm^{-1}. On the other hand, there are only two LBMs with a separation of ~45 cm^{-1} (Figure 3b). With respect to electronic resonances, we follow the same analysis as for 2LG to define phonon momenta k_{max} and k_{min} (Figure 3b) for the different electronic resonances in ABC-stacked 3LG (see Supporting Information for details). We find that the energies of the LO+ZO′ phonons for k_{max} and k_{min} differ by 20 cm^{-1}, consistent with the experimental observations of the peak splitting.

The experimental data also provide evidence of the role of the various LBM branches in FLG in defining the peaks in the LOZO′ band. In particular, for FLG with $N > 3$ the separation between the peaks within the LOZO′ band becomes comparable to the energy splitting of the LBM branches. Also the frequencies of all the subpeaks (Figure 4b) evolve systematically with the layer number as expected for the different LBM branches in FLG. For a more quantitative analysis, we estimate the energies of the LBM branches in FLG within a scheme of graphene layers interacting through identical nearest-neighbor couplings. Note that adjacent graphene layers have the same local stacking for both AB and ABC structures, so that we predict within this model the same behavior for both stacking orders. Neglecting the finite in-plane wave vector, this problem is just that of oscillations of N masses connected by $N - 1$ springs. The mode frequencies are thus $\omega_n(N) = \omega_o \sin(n\pi/2N)$, where the integer $1 \leq n \leq N-1$ specifies the branch of the mode, ω_o is the frequency in the bulk limit, that is, of the LBM mode of bulk graphite. Here we set ω_o = 132.3 cm^{-1}, taken as half of the measured value of the double-resonant 2ZO′ overtone mode for graphite (see Supporting Information). As dispersion of the LBM is rather weak near the zone center (Figure 3), the inaccuracy of our estimation from the effect of in-plane phonon dispersion is small (~2 cm^{-1}).

The calculated values of $\omega_n(N)$, upshifted to account for the LO phonon energy, are displayed in Figure 4b. The results reproduce the trends and the approximate frequencies of the different LOZO′ subpeaks for the FLG samples. Some deviations are observed for the high-energy peaks of the ABC spectra, which scatter on the higher and lower sides of the theoretical curve. We assume that they are associated with the same LBM branch but different electronic resonances. We take the average of these values to compare with the model. Although more rigorous calculations are needed to investigate the detailed mechanism of the LOZO′ mode, our analysis shows that different LBM branches present for layer thickness $N > 2$ can contribute to the observed LOZO′ bands in FLG.

In conclusion, we have identified the LOZO′ combination mode Raman band for FLG of layer thickness up to $N = 6$, thus gaining access to the low-frequency layer breathing (ZO′) mode. The Raman band is found to be highly sensitive to interlayer interactions and to exhibit a unique line shape for graphene of each layer thickness and stacking order. The distinctive properties of LOZO′ mode reflect the roles of the evolution of the different LBM branches and the selection of different phonon wave vectors through the electronically resonant Raman process. The LOZO′ mode is seen to be a convenient probe of the low-energy out-of-plane interlayer vibrations and to provide an attractive new tool for noncontact characterization of both the layer number and stacking order in few-layer graphene up to at least six layers. The recent observation of the interlayer shearing mode[20] provides an alternative signature in Raman scattering for the determination of layer thickness of FLG. The shearing mode is, however, insensitive to the stacking order. The layer thickness is determined by the shift of the single observed spectral feature. Because of the low Raman shift (<80 cm^{-1}), the measurement requires somewhat specialized Raman spectrometer, gas purging because of the rotational Raman response of air, and effective suppression of substrate signals. In contrast, characterization using the LOZO′ mode can be performed under ambient conditions using standard Raman instrumentation. The highly structured features of the LOZO′ response also render this signature of layer thickness and stacking order robust against environmental perturbations such as temperature variation and strain. More generally, interlayer vibrations in other two-dimensional layered materials are of great interest. As for the case of FLG examined here, these modes are typically at low frequency and, hence, difficult to observe directly. Our research suggests that combination Raman scattering with intralayer phonons, which effectively upshifts the frequency of the interlayer modes to a more accessible spectral range, may be a valuable approach for this broader class of materials.

■ ASSOCIATED CONTENT

Ⓢ Supporting Information

The material contains details about the preparation and infrared characterization of the graphene samples; investigation of substrate effects on the Raman spectra; and Raman measurements and analysis of the weak second-order modes in 1LG, of the 2ZO′, 2LO, LOZA, and 2ZO mode in 2LG, of the LOZO′ modes in ABA and ABC stacked 3LG, and of 2ZO′ mode in bulk graphite. This material is available free of charge via the Internet at http://pubs.acs.org.

■ AUTHOR INFORMATION

Corresponding Author

*E-mail: tony.heinz@columbia.edu.

Notes

The authors declare no competing financial interest.

■ ACKNOWLEDGMENTS

We thank Y. Miyauchi and K. Sato for valuable discussions and Z. Q. Li for assistance in sample preparation. Research at

Columbia University was supported by the Office of Naval Research through the MURI program and by the National Science Foundation through grants DMR-1106225 and DMR-1122594 with additional support from the NRI program of the Semiconductor Research Corporation. R.S. acknowledges MEXT Grant 20241023, and L.M.M. acknowledges a CNPq Fellowship from Brazil.

REFERENCES

(1) Nicklow, R.; Wakabayashi, N.; Smith, H. G. *Phys. Rev. B* **1972**, *5*, 4951−4962.
(2) Mohr, M.; Maultzsch, J.; Dobardzcaronicacute, E.; Reich, S.; Miloscaronevicacute, I.; Damnjanovicacute, M.; Bosak, A.; Krisch, M.; Thomsen, C. *Phys. Rev. B* **2007**, *76*, 035439.
(3) Spudat, C.; Müller, M.; Houben, L.; Maultzsch, J.; Goss, K.; Thomsen, C.; Schneider, C. M.; Meyer, C. *Nano Lett.* **2010**, *10*, 4470−4474.
(4) Levshov, D.; Than, T. X.; Arenal, R.; Popov, V. N.; Parret, R.; Paillet, M.; Jourdain, V.; Zahab, A. A.; Michel, T.; Yuzyuk, Y. I.; Sauvajol, J. L. *Nano Lett.* **2011**, *11*, 4800−4804.
(5) Kitipornchai, S.; He, X. Q.; Liew, K. M. *Phys. Rev. B* **2005**, *72*, 075443.
(6) Yan, J.-A.; Ruan, W. Y.; Chou, M. Y. *Phys. Rev. B* **2008**, *77*, 125401.
(7) Michel, K. H.; Verberck, B. *Phys. Rev. B* **2008**, *78*, 085424.
(8) Saha, S. K.; Waghmare, U. V.; Krishnamurthy, H. R.; Sood, A. K. *Phys. Rev. B* **2008**, *78*, 165421.
(9) Jiang, J.-W.; Tang, H.; Wang, B.-S.; Su, Z.-B. *Phys. Rev. B* **2008**, *77*, 235421.
(10) Wang, H.; Wang, Y.; Cao, X.; Feng, M.; Lan, G. *J. Raman Spectrosc.* **2009**, *40*, 1791−1796.
(11) Wang, J. B.; He, X. Q.; Kitipornchai, S.; Zhang, H. W. *J. Phys. D: Appl. Phys.* **2011**, *44*, 135401.
(12) Karssemeijer, L. J.; Fasolino, A. *Surf. Sci.* **2011**, *605*, 1611−1615.
(13) Sato, K.; Park, J. S.; Saito, R.; Cong, C.; Yu, T.; Lui, C. H.; Heinz, T. F.; Dresselhaus, G.; Dresselhaus, M. S. *Phys. Rev. B* **2011**, *84*, 035419.
(14) Michel, K. H.; Verberck, B. *Phys. Rev. B* **2012**, *85*, 094303.
(15) Cong, C. X.; Yu, T.; Sato, K.; Shang, J. Z.; Saito, R.; Dresselhaus, G. F.; Dresselhaus, M. S. *ACS Nano* **2011**, *5*, 8760−8768.
(16) Thomsen, C.; Reich, S. *Phys. Rev. Lett.* **2000**, *85*, 5214−5217.
(17) Ferrari, A. C. *Solid State Commun.* **2007**, *143*, 47−57.
(18) Malard, L. M.; Pimenta, M. A.; Dresselhaus, G.; Dresselhaus, M. S. *Phys. Rep.* **2009**, *473*, 51−87.
(19) Lui, C. H.; Li, Z.; Chen, Z.; Klimov, P. V.; Brus, L. E.; Heinz, T. F. *Nano Lett.* **2011**, *11*, 164−169.
(20) Tan, P. H.; Han, W. P.; Zhao, W. J.; Wu, Z. H.; Chang, K.; Wang, H.; Wang, Y. F.; Bonini, N.; Marzari, N.; Pugno, N.; Savini, G.; Lombardo, A.; Ferrari, A. C. *Nat. Mater.* **2012**, *11*, 294−300.
(21) Mak, K. F.; Shan, J.; Heinz, T. F. *Phys. Rev. Lett.* **2010**, *104*, 176404.
(22) Mak, K. F.; Sfeir, M. Y.; Misewich, J. A.; Heinz, T. F. *Proc. Natl. Acad. Sci. U.S.A.* **2010**, *107*, 14999−15004.
(23) Lui, C. H.; Li, Z.; Mak, K. F.; Cappelluti, E.; Heinz, T. F. *Nat. Phys.* **2011**, *7*, 944−947.
(24) Li, Z. Q.; Lui, C. H.; Cappelluti, E.; Benfatto, L.; Mak, K. F.; Carr, G. L.; Shan, J.; Heinz, T. F. *Phys. Rev. Lett.* **2012**, *108*, 156801.
(25) Brar, V. W.; Samsonidze, G. G.; Dresselhaus, M. S.; Dresselhaus, G.; Saito, R.; Swan, A. K.; Uuml; nl, S., M.; Goldberg, B. B.; Souza Filho, A. G.; Jorio, A. *Phys. Rev. B* **2002**, *66*, 155418.
(26) Cong, C.; Yu, T.; Saito, R.; Dresselhaus, G. F.; Dresselhaus, M. S. *ACS Nano* **2011**, *5*, 1600−1605.
(27) Rao, R.; Podila, R.; Tsuchikawa, R.; Katoch, J.; Tishler, D.; Rao, A. M.; Ishigami, M. *ACS Nano* **2011**, *5*, 1594−1599.
(28) Saito, R.; Jorio, A.; Souza Filho, A. G.; Dresselhaus, G.; Dresselhaus, M. S.; Pimenta, M. A. *Phys. Rev. Lett.* **2001**, *88*, 027401.